CHAPTER 6

Multi-Objective Evolutionary Design of Adenosine Receptor Ligands

This chapter is based on:

van der Horst, E.; Marqués-Gallego, P.; Mulder-Krieger, T.; van Veldhoven, J.; Kruisselbrink, J.; Aleman, A.; Emmerich, M. T. M.; Müller, C. E.; Brussee, J.; Bender, A.; IJzerman, A. P. Multi-Objective Evolutionary Design of Adenosine Receptor Ligands. [Submitted]

6.1 Abstract

A novel multi-objective evolutionary (MOE) *de novo* design method was developed and applied in this chapter to the discovery of new antagonists for the A_1 adenosine receptor. This method consists of several iterative cycles of structure generation, evaluation and selection. We applied an evolutionary algorithm (the so-called Molecule Commander) to generate candidate A_1 adenosine receptor antagonists, which were evaluated against multiple criteria and objectives consisting of high (predicted) affinity and selectivity for the receptor, together with good ADMET properties. A pharmacophore model for the human A_1 adenosine receptor (hA_1AR) was created to serve as an objective function for evolution. In addition, three support vector machine models based on molecular fingerprints were developed for the other adenosine receptor subtypes (hA_{2A}, hA_{2B} and hA_3) and applied as negative objective functions, to aim for selectivity. Structures with a higher evolutionary fitness with respect to ADMET and pharmacophore matching scores were selected as input for the next generation, and thus developed towards overall fitter ('better') compounds. We finally obtained a collection of 3.946 unique compounds from which we derived chemical scaffolds. Six of these were selected for actual synthesis and subsequently tested for activity towards all adenosine receptors subtypes. Interestingly, two compounds revealed micromolar and submicromolar affinity for the adenosine receptors, namely 4.6 µM for hA_1AR and 4.8 µM for $hA_{2A}AR$ for the first scaffold, and 6.2 µM for hA_1AR, 1.8 µM for $hA_{2A}AR$, 11 µM for $hA_{2B}AR$ and 0.96 µM for hA_3AR for the second scaffold. To further investigate our evolutionary design method, we performed systematic modifications on one of these two scaffolds. We observed that an increased affinity with appreciable selectivity for hA_1AR over the other adenosine receptor subtypes was achieved through substitution of the scaffold; the compound with highest selectivity for hA_1AR had a 1.6 µM affinity for this receptor and displayed 27%, -21%, and 11% displacement for the hA_{2A}, hA_{2B}, and hA_3 receptor subtypes respectively.

6.2 Introduction

Adenosine receptors (AR) belong to the superfamily of G protein-coupled receptors (GPCRs) and are involved in signal transduction.[1, 2] Extracellular signals transduced by GPCRs include small molecules and proteins, and even photons (light). To date, four adenosine receptors have been characterized, the A_1, A_{2A}, A_{2B} and A_3 subtypes, with adenosine as their respective endogenous ligands and they are important pharmacological targets in the treatment of different disorders, such as inflammatory, CNS and cardiovascular diseases.[3] In particular, A_1 AR antagonists are thought to be potentially useful for the treatment of neurological and cardiac disorders, renal failure, edema, as cognition enhancers, and as anti-asthma bronchiolitic drugs.[4] As for all four adenosine receptors, the human A_1 AR shows a wide distribution over the body with a variety of functions, which may lead to undesired side effects. Therefore, the design and development of A_1AR-selective ligands is an ongoing challenge, where until this stage both xanthine and non-xanthine like ligands resulted in highly potent and selective A_1 AR antagonists.[5]

A core objective of our computational research program is to automate the drug design process as much as possible to present only the most suitable candidates for a biological target to the chemist. Recently, we reported a user-friendly, fully automated desktop application for *de novo* design, the 'Molecule Evaluator'.[6] An important feature of this software is that, in contrast to many *de novo* design programs, it is an interactive tool for exploring novel chemical structures, while at the same time taking into account the expertise of the medicinal chemists on the fly. This approach has already helped us in designing new molecules active at a number of biogenic amine targets, such as the imidazole and muscarinic (M_{1-5}) receptors, NE and 5-HT transport proteins, and nicotinic acetylcholine ion channel.[7]

In the present study we report the development and application of a *de novo* molecule design procedure for the automated generation of new (candidate) lead compounds using multi-objective evolutionary (MOE) optimization,[8] as implemented in the

'Molecule Commander'. The consideration of multiple bioactivities, here considered in a multi-objective optimization routine, is important for both achieving the desired efficacy[9] as well as for avoiding off-target effects[10] and it is in line with current approaches of designing also 'selectively unselective'[11] drugs, instead of only hitting single targets thought to be involved in the disease under consideration.

A schematic drawing of the multi-objective evolutionary method is provided in Figure 1, and a detailed description is reported in the Experimental Section. Our multi-objective evolutionary design procedure consists of an iterative cycle of structure generation, evaluation, and selection of candidate structures. We prospectively validated our methodology towards the design and synthesis of new A_1 AR antagonists, showing that such an approach may indeed yield active and selective ligands for a given target.

6.3 Results and discussion

6.3.1 Multi-objective evolutionary optimization.

The evolutionary loop starts by generating new candidate molecules with the Molecule Commander program (Figure 1). Like the Molecule Evoluator,[6] this command-line program creates new structures by randomly modifying or combining a set of input molecular fragments by, *e.g.*, changing atom types, extending or breaking rings, and/or adding small functional groups. In addition, simple chemical rules are applied to avoid generation of improbable structures (see experimental section for details). In addition, the program calculates a set of physicochemical properties on the fly, which are used to limit output to structures with desired properties. After structure generation toxicity prediction using a simple mutagenicity model was performed, which was a categorical Support Vector Machine (SVN) model trained on Ames-test mutagenicity data.[12] This served merely as a proof of concept at this stage, and more extensive or proprietary toxicity predictors could readily extend or replace this component. For energy

calculation, the minimized energy of a single 3D conformer was used (note that until this point, only the topology ('graphs') of the molecules was considered). Occurrence of high-energy structures, which were weeded from the total compound library, is a consequence of the random modification of the molecular graph, which may result in less feasible molecules.

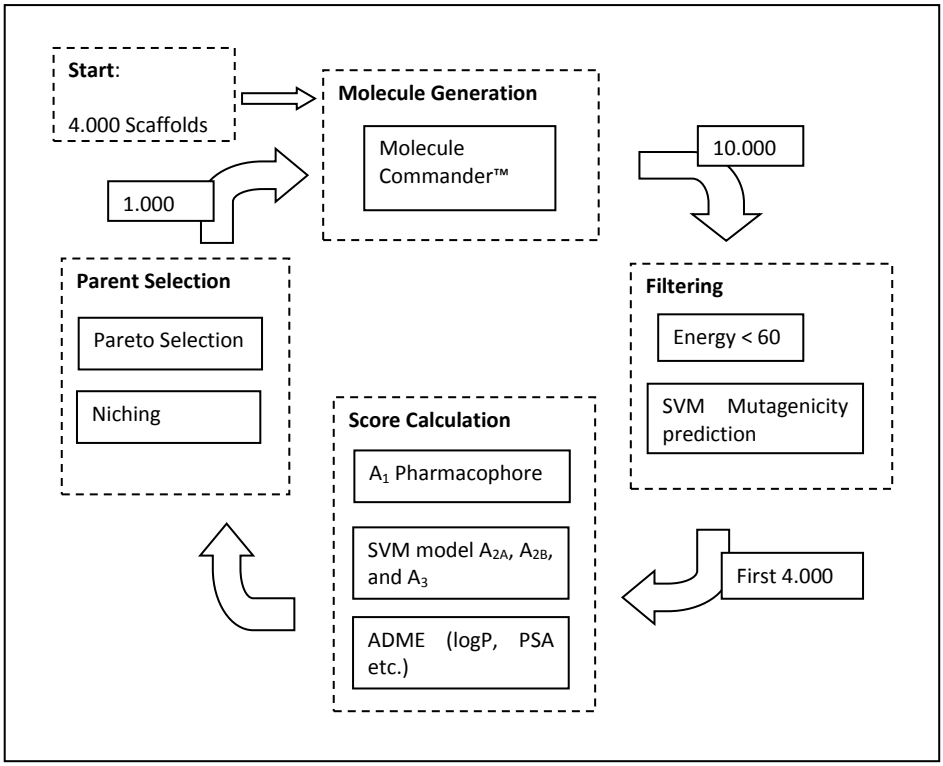

Figure 1. Flow chart of the evolutionary optimization loop (see Experimental for detailed explanation).

After the initial generation and filtering phase, the 'fittest' molecules were selected to serve as parents for the subsequent generation. To determine which molecules are 'best', several objectives were taken into account, namely high affinity, high selectivity, and good ADME properties. To predict affinity for hA_1 AR a pharmacophore model was employed that was based on a previously published pharmacophore scheme from our lab for highly potent hA_1 AR antagonists (Supporting Information Figure S1).[13] We

chose to replicate this pharmacophore model because it proved successful for the design of novel ligand chemistry with sufficient specificity. (see Figure 2 for the resulting model).

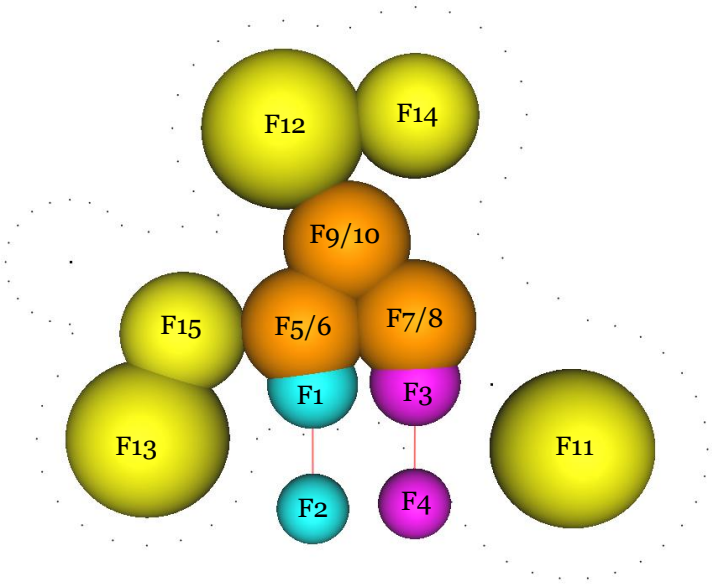

Figure 2. Visual representation of the pharmacophore model used to search for A_1 ligands, based on a previously reported pharmacophore.[13] The aromatic core is represented by three spheres F5, F7, and F9, and three spheres that indicate the direction of the normal of the aromatic feature, F6, F8, and F10. At least one of the aromatic features with normal projection should be occupied by a corresponding aromatic feature in the molecule. Three lipophilic regions are represented by spheres F11, F12/F14 and F13/F15. A hydrogen bond acceptor and donor region are represented by F1 and F3, respectively. The direction of the hydrogen bond is indicated with F2 and F4. The grey dots indicate the inclusion volume, the volume into which the molecules generated need to fit for not being subject to a fit penalty.

In contrast to the pharmacophore model used to predict affinity for the A_1 receptor, a continuous Support Vector Machine (SVM) model[14] trained on ligands of each of the other three adenosine receptor subtypes (A_{2A}, A_{2B}, and A_3) was used to estimate ligand

affinity for these receptors. The reason for this is that for the adenosine A_1 receptor the binding features needed to be defined as specific as possible, while for the other three subtypes (selectivity score) a broad range of possible ligand features had to be detected to ensure selectivity. To predict ADME characteristics, several physicochemical properties, such as solubility (logS), lipophilicity (logP) and polar surface area (PSA), were calculated. Property ranges were defined, outside of which molecules were rejected using filters. Apart from these hard cut-offs, we also included a measure that defined how close a molecule is to ideal property values for ADME. Therefore, between hard cut-offs and ideal property ranges, a gradient in ADME score was introduced to describe how close the property values are towards the ideal range, giving the algorithm a chance to improve towards good ADME properties. For this, each property was converted using a desirability function to a value between zero and one, where zero (0) indicates undesirable property values and one (1) that property values are excellent. The values of all desirability functions were combined into the desirability index, representing the ADME score. The use of desirability functions/indices originates from areas such as quality control.[15]

The three calculated scores – the affinity score, the selectivity score, and the ADME score – served as input for selecting the best parents for the next generation. This was performed with Pareto selection, which is a method to select the best candidates when considering multiple objectives.[16] In contrast to a simple combination of scores into a single score, Pareto selection considers all three scores simultaneously to select the best candidates. Since evolutionary algorithms have a tendency to focus towards small regions of the chemical search space,[17] diversity of the parent molecules was also taken into account using niching.[18] Niching enforces diversity within populations of candidate solutions by maintaining separated groups, requiring a minimum distance between those groups and a maximum distance between the group members. Distance is based on a (dis)similarity measure such as the Tanimoto index. [19]

For each new generation, the number of known structures, the number of structures with known adenosine ligand scaffolds, and the number of structures with high

pharmacophore score were calculated. When these measures reached a plateau, the process was stopped. Chart 1 shows the percentage of compounds that contain known adenosine scaffolds as well as those having a high pharmacophore score. The occurrence of scaffolds also found in adenosine ligands (which were removed) gave us some upfront confidence that the generated structures might indeed be potential adenosine receptor ligands. In general, the number of compounds with a high pharmacophore score is expected to improve over the generations while the number of unknown compounds will increase as well. Although generation of novel compounds is preferred from a medicinal chemistry point of view, a high number of unknown compounds also signals for potential difficulties with synthesis planning or acquisition of starting materials. As visualized by the 'Scaffolds' bars in Chart 1, the percentage of scaffolds also found in common adenosine receptor ligands decreases with each generation. The data presented in Chart 1 also suggests that the pharmacophore fit improves with each subsequent generation; the first generated compounds with at least 13 pharmacophore matches first appear in the fifth generation.

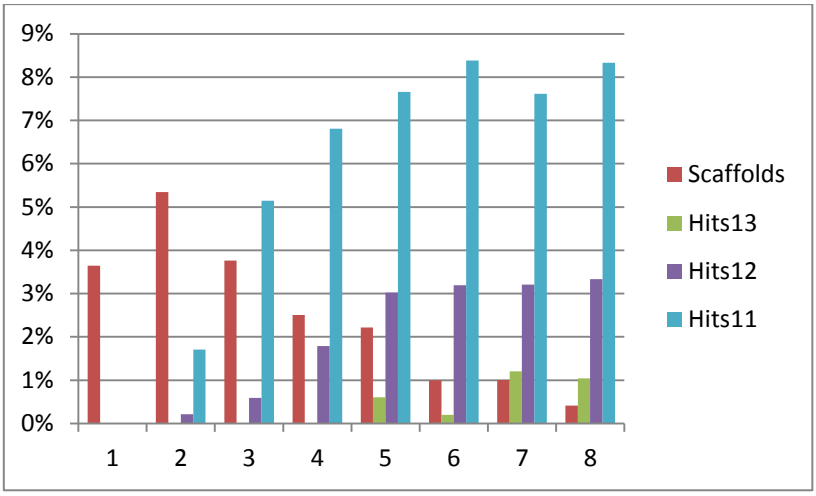

Chart 1. Percentage of compounds that contain known adenosine ligand scaffolds ("Scaffolds"), and the percentage of compounds with at least 11, 12, or 13 pharmacophore feature hits ("Hits11"/"Hits12"/"Hits13") per generation (number of generations on X-axis).

The generated molecules from all generations were collected and merged into one set (discarding duplicates), resulting in a set of 3.946 unique structures. From this set, structures with high pharmacophore score, *i.e.* at least 11 matching pharmacophore points, were selected. The resulting set of 242 hits was examined for novelty by matching the structures against a set of common adenosine receptor scaffolds and ring systems. 43 molecules that had a common AR scaffold or ring system at their core were discarded (provided in Figure S2 in Supporting Information), yielding a final set of 199 novel candidates. These candidates were grouped by scaffold and ranked according to pharmacophore score, as provided in Figure S3 of Supporting Information, to aid further manual inspection.

As mentioned above, different structures not known to be adenosine receptor ligands were generated and clustered into different groups (*i.e.* substituted 6:6:5, 6:6:6, or 5:5:6 fused heteroaromatic systems, substituted imidazoles, triazoles, tetrazoles and quinazolinediones), which demonstrate the variety and diversity of the chemistry

provided by our multi-objective evolutionary method (see Supporting Information, Figure S4). We observed that all these scaffolds contained substituents of different nature, at different positions on the scaffold.

6.3.2 Chemistry and Biological Evaluation.

To investigate the qualities of the multi-objective evolutionary design method, we began with the preparation of six scaffolds (Figure 3), the selection of which was based on ease of synthesis according to a panel of in-house medicinal chemists. Moreover, we were interested in the influence of the suggested substituents; therefore, we began with simple substitution (methyl groups) if any on these six scaffolds.

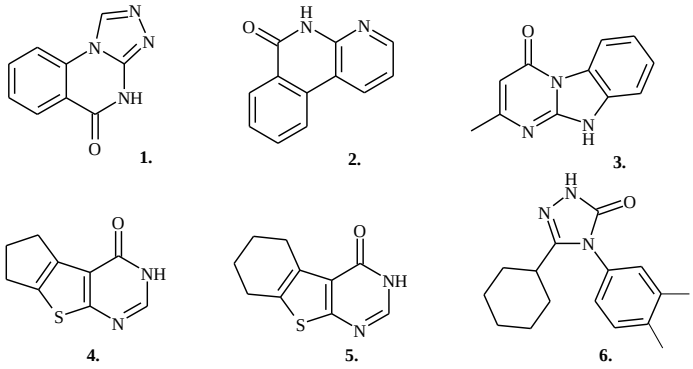

Figure 3. Chemical structures of selected scaffolds generated using the multi-objective evolutionary design method: [1,2,4]Triazolo[4,3-a]quinazolin-5-one (**1**), 4-Aza-5[*H*]-phenanthridin-6-one (**2**), 2-Methylpyrimido[1,2-a]benzimidazol-4(10*H*)-one (**3**), 3,5,6,7-Tetrahydro-4*H*-cyclopenta[4,5]thieno[2,3-d]pyrimidin-4-one (**4**), 5,6,7,8-Tetrahydro[1]benzothieno[2,3-d]pyrimidin-4(3*H*)-one (**5**). 5-Cyclohexyl-4-(3,4-dimethylphenyl)-2,4-dihydro-3*H*-1,2,4-triazol-3-one (**6**).

The 6:6:5 fused heteroaromatic system [1,2,4]triazolo[4,3-a]quinazolin-5-one (**1**) was synthesized as previously reported,[20] by the cyclization of 2-hydrazinoquinazolin-4-one[21] in formic acid. Compound **2** was synthesized using a slightly modified reported

method,[22] starting from the synthesis of the 2-(*N,N*-diisopropylcarboxamido)phenylboronic acid,[23] which was then used in a Suzuki-Miyaura cross-coupling reaction with 2-amino-3-bromopyridine under microwave conditions. Subsequently, cyclization of 2-(2-aminopyridin-3-yl)-*N,N*-diisopropylbenzamide using lithium diisopropylamide yielded the desired compound **2**. The 6:5:6 fused heteroaromatic system 2-methylpyrimido[1,2-*a*]benzimidazol-4(10*H*)-one (**3**) was obtained by heating a mixture of 2-aminobenzimidazole and ethyl acetoacetate in the presence of phosphoryl chloride and phosphoric acid. The free base (**3**) was liberated by the addition of $NaHCO_3$. [22] Both substituted 2-aminothiophenes (2-amino-5,6-dihydro-4*H*-cyclopenta[*b*]thiophene-3-carbonitrile and 2-amino-4,5,6,7-tetrahydro-1-benzothiophene-3-carbonitrile) were synthesized using Gewald's method, which involves condensation of the corresponding ketone (cyclopentanone or cyclohexanone) with an activated nitrile and elemental sulfur in the presence of KF/alumina as catalyst.[24] Cyclization of 2-amino-5,6-dihydro-4*H*-cyclopenta[*b*]thiophene-3-carbonitrile and 2-amino-4,5,6,7-tetrahydro-1-benzothiophene-3-carbonitrile in formic acid at 110 °C yielded compounds **4** and **5**, respectively Compound **6** was synthesized starting from the commercially available 3,4-dimethylphenylisocyanate, which was reacted with hydrazine hydrate to obtain the corresponding semicarbazide, and was subsequently condensed with cyclohexanecarboxaldehyde to afford the corresponding semicarbazone. Finally, alkaline potassium ferricyanide oxidation of this semicarbazone yielded the desired compound **6**. Schemes showing the synthesis path and reaction conditions are in the Supporting Information (Schemes S1-S5).

All these compounds (**1**-**6**) were tested in the radioligand binding assays at human A_1 ([^{3}H]DPCPX), A_{2A} ([^{3}H]ZM241385), A_{2B} ([^{3}H]PSB603) and A_3 receptors ([^{3}H]PSB11 or [^{125}I]AB-MECA). Initially, all compounds were screened at a single concentration of 10 µM on all four receptor subtypes. For compounds that inhibited radioligand binding for more than 30% at one or more receptor subtypes the K_i values were subsequently determined (Table 1).

Table 1. Affinities and % displacement values of compound **1-6** in Radioligand Binding Assays at human Adenosine Receptors

	Ki±SEM (μM, n=3) (or % displacement at 10 μM, average of n=2)			
Compd	**hA_1[a]**	**hA_{2A}[b]**	**hA_{2B}[c]**	**hA_3[d]**
1	0%	0%	11%	3%
2	4.6±1.5	4.8±2.3	13%	4%
3	6.2±1.3	1.8±0.3	11±1	0.96±0.17
4	3%	0%	5%	1%
5	13%	-12%	12%	-1%
6	9%	-1%	1%	6%

[a] Displacement of specific [^{3}H]DPCPX binding from CHO cell membranes expressing human adenosine A_1 receptors or % displacement of specific binding. [b] Displacement of specific [^{3}H]ZM241385 binding from HEK 293 cell membranes expressing human adenosine A_{2A} receptors or % displacement of specific binding. [c] Displacement of specific [^{3}H]PSB603 binding from CHO cell membranes expressing human adenosine A_{2B} receptors or % displacement of specific binding. [d] Displacement of specific [^{3}H]PSB11 binding from CHO cell membranes expressing human adenosine A_3 receptors or % displacement of specific binding.

As summarized in Table 1, two of the six scaffolds showed activity towards at least two of the adenosine receptor subtypes, including the hA_1 AR. Compound **2** had micromolar affinity for both A_1 and A_{2A} ARs. Compound **3** appeared active on all four adenosine receptor subtypes, also in the micromolar range. We were happy with the 33% 'hit rate', but concluded at the same time that the evolution of chemistry towards A_1 receptor selectivity was only partially successful. This may have to do with our simplification of suggested molecules towards unsubstituted scaffolds only, or that the SVM methods for our 'off-targets' of A_{2A}, A_{2B} and A_3AR were not robust enough. As a next step we decided therefore to perform a systematic modification by substitution of the novel 6:5:6-fused scaffold **3** to investigate a possible enhancement of affinity and subtype selectivity for the hA_1AR.

Inspection of the generated molecules that contained this 10*H*-pyrimido-[1,2-*a*]-benzimidazol-4-one scaffold, revealed that the insertion of a simple alkyl chain at the

R^3 position of the scaffold lead to high-scoring molecules. Therefore, we replaced the methyl group on scaffold **3** by different alkyl groups (Figure 4) and investigated the influence thereof on adenosine receptor affinity. A series of compounds were synthesized (**3a-3k**) by reacting the corresponding 2-aminobenzimidazole with the appropriate β-keto-ester under microwave conditions (see Supporting Information). All derivatives were tested in radioligand binding studies starting at either 10 μM or 1 μM concentrations on the A_1 AR. To determine the selectivity of these derivatives for the A_1 AR the interaction with the other AR subtypes (A_{2A}, A_{2B} and A_3) were also investigated. For those derivatives that gave more than 50% displacement at 1 μM concentration, whole displacement curves were recorded to determine the K_i value of each compound. In Table 2, both % displacement and K_i values for each derivative are summarized.

We observed that increasing bulkiness by introducing an *iso*-propyl group at the R^3 position (**3a**) yielded improved affinity on the hA_1 AR, with a K_i value of 0.28 ±0.06 μM, 22-fold lower than the K_i value of parent scaffold **3** (Table 2), and also better selectivity towards the hA_1 AR. A linear propyl group at the R^3 position (**3b**) also improved the K_i value compared to compound **3**, but less so than the *iso*-propyl substituent. These findings prompted us to synthesize the cyclohexyl derivative **3c**, which provides an even bulkier substituent at the R^3 position, yet not aromatic. Although not elaborated further **3c** showed 49% displacement at 1 μM on the hA_1 AR, suggesting a K_i value in the low micromolar region, similar to that found for the propyl derivative **3b**. Subsequently, aromatic rings were also explored as substituents at the R^3 position, introducing an additional planar lipophilic domain on the structure. As listed in Table 2, inserting a phenyl ring at the R^3 position lead to compound **3d** with highest affinity on the A_1 receptor, with a K_i value of 0.13±0.05 μM, although selectivity was lost toward both hA_{2B} and hA_3 AR. 4-Pyridyl substitution **3e** lead to a less active compound (43% displacement of [^{3}H]DPCPX radioligand binding at 1 μM).

Modifications on both R^1 and R^2 positions on the 10*H*-pyrimido-[1,2-*a*]-benzimidazole-4-one scaffold were also investigated. Interestingly, introducing methyl groups on both

R^1 and R^2 positions decreased interaction with the adenosine receptors (Table 2). A pronounced example of this observation is compound **3g** compared to its analogue **3a**, displaying an almost 6-fold lower affinity for the hA_1 AR. Compound **3g** has negligible affinity for the other adenosine receptor subtypes with low % displacement on A_{2A}, A_{2B} and A_3 AR at 1 μM concentration (27%, - 21% and 11%, respectively). Therefore, the combination of R^3 = *i*-Pr and R^1 = R^2 = Me yielded the most selective compound of this series.

Interestingly, compound **3g** was also directly suggested from the *de novo* design procedure, indicative of the predictive power of the method.

Table 2. Affinities or % displacement of compounds **3a-3k** in Radioligand Binding Assays at human Adenosine Receptors.

R^1 = H, Me

R^2 = H, Me

R^3 = Me, *i*-Pr, Pr, *c*-Hex, Ph, 4-Py

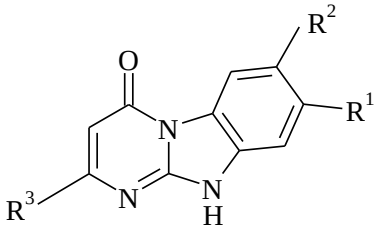

3a-k

compd				K_i±SEM (μM, n=3) (or % displacement at 1 μM, average of n=2)[a]			
	R^1	R^2	R^3	hA_1[b]	hA_{2A}[c]	hA_{2B}[d]	hA_3[e]
3	H	H	Me	6.2±1.3	1.8±0.3	11±1	0.96±0.17
3a	H	H	*i*-Pr	0.28±0.06	2.4±0.6	19%	-11%
3b	H	H	Pr	1.3±0.3	3.6±0.6	25%	17%
3c	H	H	*c*-Hex	49%	48%	-29%	23%
3d	H	H	Ph	0.13±0.05	43%	0.52±0.18	0.15±0.04
3e	H	H	4-Py	45%	20%	8%	18%
3f	Me	Me	Me	27%	1.7±0.5	-36%	15%
3g	Me	Me	*i*-Pr	1.6±0.5	27%	-21%	11%
3h	Me	Me	Pr	40%	27%	-4%	15%
3i	Me	Me	*c*-Hex	-1%	-5%	-22%	12%
3j	Me	Me	Ph	0.59±0.18	0%	-14%	1.6±0.7
3k	Me	Me	4-Py	10%	0%	-[f]	12%

[a] K_i (SEM (n = 3), % displacement (n=2) at 1 μM. [b] Displacement of specific [^{3}H]DPCPX binding in CHO cells expressing human adenosine A_1 receptors or % displacement of specific binding. [c] Displacement of specific [^{3}H]ZM241385 binding in HEK 293 cells expressing human adenosine A_{2A} receptors or % displacement of specific binding concentrations. [d] Displacement of specific [^{3}H]PSB603 binding in CHO SNAP cells expressing human adenosine A_{2B} receptors or % displacement of specific binding. [e] Displacement of specific [^{125}I]AB-MECA binding in HEK 293 cells expressing human adenosine A_3 receptors or % displacement of specific binding. [f] solubility issues precluded a determination.

6.4 Conclusions

We developed a *de novo* multi-objective evolutionary design procedure and applied it to adenosine receptors, a subclass of the superfamily of G protein-coupled receptors. This method provides the user with a fast and automated generation of best candidate structures and close analogues thereof. Significant micromolar affinity was obtained with two (out of six) scaffolds that were generated in the design process, 4.6 and 4.8 μM for respectively hA_1AR and $hA_{2A}AR$ for the first scaffold, and 6.2, 1.8, 11, and 0.96 μM for respectively hA_1AR, $hA_{2A}AR$, $hA_{2B}AR$, and hA_3AR for the second scaffold, showing its versatility and relatively high 'hit rate'. Moreover, systematic modifications based on the generated structures resulted in an improved affinity and selectivity towards the A_1 adenosine receptor, the primary target of interest in our study. For instance, the compound with highest selectivity for hA_1AR had a 1.6 μM affinity for this receptor and displayed 27%, -21%, and 11% displacement for the hA_{2A}, hA_{2B}, and hA_3 receptor subtypes respectively In more general terms, an automated design strategy that optimizes multiple parameters simultaneously appeared feasible and attractive as it allows an unbiased exploration of chemical space. We anticipate that novel scaffolds for other targets can be derived in a similar way, thus helping the medicinal chemists in their drug discovery efforts.

6.5 Experimental Section

6.5.1 Reference Ligands

For analysis and model generation, sets of reference ligands for the human adenosine receptor subtypes were retrieved from the ChEMBL database.[25] Query parameters for database retrieval were 'Confidence' of 5 or higher (7 being the highest), only direct relationships and only binding assays. Ligands with pK_i values of 5.0 or higher were used, resulting in a set of 633 ligands for A_{2A}, 439 ligands for A_{2B}, and 985 ligands for A_3 human adenosine receptor subtypes.

6.5.2 Evolutionary Optimization Loop

As input for the first generation of structures, a starting set of 4000 of the most common scaffolds extracted from the purchasable compound set from ZINC (version 8, http://zinc.docking.org, accessed July 2009)[26] was used. Here, a scaffold was defined as the collection of ring atoms and bonds, and linker atoms and bonds connecting these rings.[27, 28] Atoms doubly-bonded to the scaffold were retained since these often have a major influence on the electronic properties of the scaffold. Structures were generated using the Molecule Commander version 4.2. The program was executed with the following filters enabled: the topological polar surface area[29] was kept between 0 Å² and 140 Å², calculated LogP between -5 and 5, molecular weight between 200 Da and 700 Da, hydrogen bond donors between 1 and 5, hydrogen bond acceptors between 1 and 10, rotatable bonds between 0 and 5, and aromatic substituents between 1 and 10. In addition, the NCI Rings filter was enabled without considering the specific (heavy) atom type. High-energy structures were filtered out by first generating 3D coordinates followed by energy minimization using Pipeline Pilot's 'Generate 3D Coordinates' and 'Minimize Energy' components.[30] Energy minimization was performed with default values for all parameters (MaximumNumberOfSteps=1000; ConvergenceEnergyDifference=0.0001). Structures possessing a minimized energy above 60 energy units (arbitrary units) were discarded. For the prediction of mutagenicity of generated compounds, a categorical support vector machine model was trained on a set of mutagenic and non-mutagenic compounds using ECFP_2 fingerprints (Pipeline Pilot).[12]

6.5.3 SVM Models for Adenosine Receptor Subtypes

To predict selectivity of the generated compounds, three continuous SVM models were trained using Pipeline Pilot ECFP 6 fingerprints for ligands of the human adenosine receptor subtypes A_{2A}, A_{2B}, and A_3. Circular fingerprints of this type have previously been shown to be among the best descriptors capturing molecular features related to bioactivity.[32] Compound training sets were retrieved from ChEMBL (see

above). As background set for training, the Maybridge compound collection included in Pipeline Pilot containing 55,000 compounds was used.

6.5.4 Pharmacophore Creation

The pharmacophore used in this study was based on a pharmacophore scheme previously proposed by Chang *et al.*[13] This pharmacophore scheme, provided in Figure S2, consists of an aromatic core surrounded by three lipophilic domains with two hydrogen bond donors and one acceptor, and it had been successfully used to design new adenosine A_1 receptor antagonists. The best compounds from the resulting series have been used in the current study to reconstruct the pharmacophore scheme of Chang *et al.*[13], namely high-affinity compounds N-(2,6-diphenylpyrimidin-4-yl)cyclopentanecarboxamide (LUF5740), N-(2,6-diphenylpyrimidin-4-yl)-2-methylbutanamide (LUF5767), and N-(4,6-diphenylpyrimidin-2-yl)butanamide (LUF5735).The hydrogen of the amide bond and the nitrogen of the pyrimidine ring form the hydrogen bond donor and acceptor part. After aligning these features, the aromatic core and lipophilic domains, Lip_1, Lip_2, and Lip_3 were defined. The second hydrogen bond acceptor, corresponding to the carbonyl group in the amidopyrimidines, was omitted since its position and direction could not reliably be derived from the reference compounds. The compounds of the reference set from Chang *et al.*[13] were used to refine the pharmacophore and further define the included volume. The resulting pharmacophore consisted of 15 features of which four were marked essential, namely the hydrogen bond donor and acceptor and corresponding projections (direction) of these features in space. The visual representation of this pharmacophore is provided in Figure 2. Note that, except for the π-ring normal projections, all features are positioned in one plane.

The pharmacophore score was defined as the number of pharmacophoric features in the molecule that match pharmacophore centers in the model, from which the root mean square distance between the feature centers in molecule and pharmacophore is subtracted. A score of zero was assigned to structures with less than eight matches.

For pharmacophore creation and compound scoring, Chemical Computing Group's Molecular Operating Environment version 2008.10 was used.[31]

6.5.5 Desirability indices

The adenosine subtype scores as well as properties values were combined into single measures named desirability indices (more specifically: linear Deringer desirability indices), which quantify the level in which individual criteria are met.[33] These indices are calculated as follows: each property is transformed into a desirability function that expresses how well criteria are met. Desirability functions have a value ranging from zero to one, where zero (0) indicates that criteria are violated and one (1) that all criteria are entirely satisfied The function displays a gradual rise between zero and one, the shape of which can vary (linear in this study), to express improvement and to steer evolution towards satisfying the criteria. Desirability functions are either one-sided or two-sided, depending on whether maximization of a value is required or whether the value should be within a specified target range. The individual desirability functions are combined into a desirability index by multiplication. For the subtype desirability index (selectivity), the desirability functions were transformed from the SVM model score for the adenosine receptor subtypes. A SVM model score below 0.2 indicated that affinity was not predicted for the adenosine receptor subtype, resulting in a desirability value of zero, while a score above 0.8 indicated predicted affinity for a subtype, resulting in a desirability value of one. Between 0.2 and 0.8, the value of the desirability function scaled linearly with the SVM model score. These values where then inverted (one minus the desirability value) and combined into the final desirability index that was used as objective.

6.5.6 Pareto Selection and Niching

A new set of candidates was selected using Pareto selection and niching.[18] Pareto selection is a method to select the set of best solutions of a problem with multiple (conflicting) objectives. The best or non-dominated solutions are those for which no

other solution is superior in all properties. The non-dominated solutions form the Pareto front and have the characteristic that it is not possible to improve on one property without degrading another property. Removing the solutions on the first Pareto front will expose the second Pareto front, removing those will expose the third, etc. Molecules are ranked according to the Pareto front from which they originate. From the top-ranked structures, diverse subsets were selected using dynamic peak identification, or 'niching',[34] whereby the best molecules are grouped in niches based on a similarity measure such as fingerprint distance. Here we used ECFP_6 fingerprints with the Tanimoto coefficient as a distance measure. Niching starts by assigning the best molecule from the Pareto selection as the first niche center. The second best molecule is compared to this niche center and if the fingerprint distance is within a set minimum known as the niche radius, it is assigned to the niche; if it falls outside the niche radius, it will be the niche center of the second niche. If the maximum number of molecules per niche is reached, the niche with the second best niche center is considered, then the third, and so on. If the molecule falls not within any of the niches and the maximum number of niches is reached, it is discarded. This process continues until all molecules are processed or all niches have the maximum number of molecules. The settings used in this experiment were: a niche radius of 0.85, with a maximum of 5 molecules per niche and a maximum of 200 niches per generation.

6.5.7 Analysis of Generated Structures

For each generation, the number of known molecules, the occurrence of scaffolds of adenosine receptor ligands, and the number of molecules with high pharmacophore score were determined. To assess the number of known molecules, presence in ZINC was checked for the generated molecules.

6.6 Materials and Methods

6.6.1 Final Candidate Selection

Generated molecules from all generations were collected and molecules with a pharmacophore score below 11 were removed. The remaining molecules were grouped by scaffold and ordered by pharmacophore score. To keep only novel candidates for further synthesis, molecules containing ring systems or scaffolds also found in adenosine receptor ligands were removed. For this, ring systems and scaffolds were extracted from the adenosine ligands in ChEMBL (see above). Single rings and fragments without heteroatoms were removed; the rest of the fragments was used for filtering. This final pruning process yielded a collection of novel scaffolds presented in Figure S1. Subsequently our chemists searched for possible routes of synthesis and availability of starting materials. Synthesis that required costly or hazardous materials was not considered further. Based on ease-of-synthesis, logS, logP, and PSA values, a final set of candidates was selected for synthesis.

6.6.2 Chemistry

All reagents were obtained from commercial sources and all solvents were of analytical grade. ^{1}H and ^{13}C NMR spectra were recorded on a Bruker AC 400 spectrometer or on a 300 MHz Bruker DPX300 spectrometer. Chemical shifts are reported in δ (ppm) and the following abbreviations are used: s = singlet, d = doublet, dd = double doublet, dt = double triplet, t = triplet, td = triple doublet, m = multiplet, br = broad. C, H and N analyses were performed with a Perkin-Elmer 2400 series II analyzer and are within 0.5% of the theoretical values unless otherwise stated. Reactions were routinely monitored by TLC using Merck silica gel F254 plates. Microwave reactions were performed on an Emrys Optimizer (Biotage AB). Wattage was automatically adjusted to maintain the desired temperature. HPLC purity of compounds was measured with a reverse-phase column (RP18, 125 x 4 mm, 5 µm, 254 nm and diode array, 210-360 nm) with two diverse solvent systems; A: Water, 10% acetonitrile, 10 mM HOAc, 5 mM SDS.

B: Water, 90% acetonitrile, 10 mM HOAc, 5 mM SDS. Samples were eluted by a gradient between 100% A and 100% B at a flow rate of 0.6 mL/min. Reverse-phase HPLC revealed that all samples submitted for assay accounted for > 95% of the UV absorbing material.

6.6.2.1 [1,2,4]Triazolo[4,3-a]quinazolin-5-one (1) [20]

2-Hydrazinoquinazolin-4-one (1g, 5.7 mmol), synthesized as previously reported,[21] was heated in formic acid (6 mL) for 4 h on a steam bath. Subsequently, the reaction mixture was cooled and poured into water to precipitate the desired compound. Yield 39% (413 mg). ^{1}H NMR (DMSO-d_6) δ = 12.82 (s, br, 1H, NH), 9.41 (s, 1H), 8.16 (m, 2H), 7.92 (t, J = 7.6 Hz, 1H), 7.57 (t, J = 7.6 Hz, 1H) ppm. ^{13}C-NMR δ (DMSO-d_6) δ = 159.7, 146.7, 134.9, 133.2, 128.6, 126.5, 117.2, 115.9 ppm. Anal. for [$C_9H_6N_4O$] found (calculated) %: C 57.8 (58.1), H 3.4 (3.3), N 30.0 (30.1). HRMS (m/z) = 187.06129 calculated for $[M+H]^+$ = 187.06144.

6.6.2.2 4-Aza-5[H]-phenanthridin-6-one (2).[22]

Suzuki-Miyaura cross-coupling reaction between 2-(*N,N*-diisopropylcarboxamido)phenylboronic acid and 2-amino-3-bromopyridine under microwave conditions was performed to obtain 2-(2-aminopyridin-3-yl)-*N,N*-diisopropylbenzamide, with subsequent cyclization affords the entitle compound 2. Briefly, 2-(*N,N*-diisopropylcarboxamido)phenylboronic acid (600 mg, 2.4 mmol), prepared according to the literature,[23] was added to a solution of 2-amino-3-bromopyridine (380 mg, 2.2 mmol), potassium carbonate (400 mg,), palladium(II) acetate (98 mg, 0.44 mmol) and triphenylphosphine (231 mg, 0.88 mmol) in toluene/ethanol/water (2:1:1) mixture. The reaction vial was then sealed and heated at 160 °C for 30 min. Upon completion the reaction mixture was poured into water and the product was extracted with ethyl acetate. The organic phases were collected and dried with $MgSO_4$ and concentrated to yield 2-(2-aminopyridin-3-yl)-*N,N*-diisopropylbenzamide as a yellow solid that was triturated with diethyl ether. The cyclization of 2-(2-aminopyridin-3-yl)-*N,N*-diisopropylbenzamide (195 mg, 0.7 mmol) was performed as previously reported,[22] with lithium diisopropylamide (1.6 M, 1.1 mL)

dissolved in 9 mL of dry THF at -78 °C. The reaction mixture was warmed to room temperature and stirred overnight. The reaction mixture was concentrated in vacuo and suspended in water (20 mL). The solid was filtered off and triturated with ethyl acetate. The resulting solid was dried yielding the desired compound. Yield 60% (82 mg). ^{1}H NMR (DMSO-d_6) δ = 12.05 (s br, 1H, NH), 8.84 (dd, J = 6.4 Hz, J = 1.6 Hz, 1H), 8.55 (d, J = 8.4 Hz, 1H), 8.50 (dd, J = 3.2 Hz, J = 1.6 Hz, 1H), 8.33 (dd, J = 6.8 Hz, J = 0.8 Hz, 1H), 7.89 (td, J = 8.2 Hz, J = 1.2 Hz, 1H), 7.69 (td, J = 7.2 Hz, 1H), 7.33 (m, 1H) ppm. ^{13}C NMR (DMSO-d_6) δ = 165.7, 163.8, 141.2, 134.9, 132.7, 128.5, 127.9, 125.9, 72.9, 22.1 ppm. Anal. for $[C_{12}H_8N_2O]\cdot H_2O$ found (calculated) %: C 67.6 (67.3), H 4.2 (4.7), N 12.9 (13.1). HRMS (m/z) = 197.07084 calculated for $[M+H]^+$ = 197.07094.

6.6.2.3 2-Methylpyrimido[1,2-a]benzimidazol-4(10H)-one (3).[35]

A mixture of 2-aminobenzimidazole (1.33 g, 0.01 mol) and ethyl acetoacetate (1.27 mL, 0.01 mol) was heated at 130 °C in phosphoryl chloride (6.13 g, 0.04 mol) and phosphoric acid (700 mg) until evolution of HCl(g) ceased. The reaction was cooled to 80 °C and subsequently ethanol was added. The reaction mixture was cooled to 0 °C to obtain a precipitate. The solid was filtered off and the free base was liberated by the addition of $NaHCO_3$ solution. The resulting solid was recrystallized from ethanol yielding the desired compound. Yield: 34% (670 mg) ^{1}H NMR (DMSO-d_6) δ = 8.35 (d, J = 7.6 Hz, 1H), 7.50 (d, J = 8.0 Hz, 1H), 7.39 (td, J = 8.4 Hz, J = 1.2 Hz, 1H), 7.24 (td, J = 8.0 Hz, J = 1.2 Hz, 1H), 5.78 (s, 1H), 2.31 (s, 3H) ppm. ^{13}C-NMR (DMSO-d_6) δ = 165.7, 163.8, 141.2, 134.9, 132.7, 128.5, 127.9, 125.9, 72.9, 22.1 ppm. HRMS (m/z) = 200.08173 calculated $[M+H]^+$ = 200.08184. Purity (HPLC) 98%.

Compounds **3a**-**3k** were synthesized under microwave conditions, which is further detailed in the Supporting Information.

6.6.2.4 3,5,6,7-Tetrahydro-4H-cyclopenta[4,5]thieno[2,3-d]pyrimidin-4-one (4)

2-Amino-5,6-dihydro-4*H*-cyclopenta[*b*]thiophene-3-carbonitrile was prepared following the typical Gewald reaction between cyclopentanone (10 mmol), malononitrile (10 mmol), sulfur (10 mmol) and KF/alumina as catalyst in EtOH under

microwave conditions.[24] 2-Amino-5,6-dihydro-4*H*-cyclopenta[*b*]thiophene-3-carbonitrile (129 mg, 0.8 mmol) and formic acid (5 mL) were heated under microwave condition for 3 min at 110 °C. The reaction mixture was cooled, poured into water, filtered and dried. Yield 41% (63 mg). ^{1}H NMR (DMSO-d_6) δ = 11.77 (s, 1H, NH), 8.44 (s, 1H), 2.90 (t, J = 7.2 Hz, 2H), 2.79 (t, J = 7.2 Hz, 2H), 2.35 (m, 2H) ppm. ^{13}C-NMR (DMSO-d_6) δ = 157.6, 30.0, 28.7, 28.3 ppm. Anal. for $[C_9H_8N_2SO]\cdot H_2O$ found (calculated) %: C 50.8 (51.4), H 4.9 (4.8), N 13.4 (13.3), S 15.3 (15.3). HRMS (m/z) = 211.05365 calculated for $[M+H_2O+H]^+$ = 211.05357.

6.6.2.5 5,6,7,8-Tetrahydro[1]benzothieno[2,3-d]pyrimidin-4(3H)-one (5)

2-Amino-4,5,6,7-tetrahydro-1-benzothiophene-3-carbonitrile was prepared following the typical Gewald reaction between cyclohexanone (0.01 mol), malononitrile (0.01 mol), sulfur (0.01 mol) and KF/alumina as catalyst in EtOH under microwave conditions.[24] 2-Amino-4,5,6,7-tetrahydro-1-benzothiophene-3-carbonitrile (200 mg, 1.1 mmol) and formic acid (5 mL) were heated under microwave condition for 3 min at 110 °C. The reaction mixture was cooled, poured into water, filtered and dried. Yield 45% (103 mg). ^{1}H NMR (DMSO-d_6) δ = 11.34 (s, 1H, NH), 8.37 (s, 1H), 2.63 (m, 4H), 1.72 (m, 4H) ppm. ^{13}C-NMR (DMSO-d_6) δ = 157.6, 26.6, 24.7, 22.7 ppm. Anal. for $[C_{10}H_{10}N_2SO]\cdot H_2O$ found (calculated) %: C, 53.4 (53.6), H 5.3 (5.4), N 12.6 (12.5), S 13.8 (14.3). HRMS (m/z) = 225.06935 calculated for $[M+H_2O+H]^+$ = 225.06922.

6.6.2.6 5-Cyclohexyl-4-(3,4-dimethylphenyl)-2,4-dihydro-3H-1,2,4-triazol-3-one (6)

Commercially available 3,4-dimethylphenylisocyanate (1 g, 6.8 mmol) was added to a solution of hydrazine hydrate (10 mmol) in 25 mL of dichloromethane at -60 °C. The reaction mixture was allowed to reach room temperature and stirred for additional 4 h. The precipitate was filtered and washed with cold dichloromethane yielding the corresponding semicarbazide. This semicarbazide (500 mg, 2.8 mmol) was then mixed with cyclohexanecarboxaldehyde (2.5 mmol, 194 µL) in ethanol (15 mL) and heated under reflux for 2 h. Subsequently, the reaction mixture was filtered and the ethanol was removed under vacuo yielding the corresponding cyclohexanecarboxaldehyde *N*-phenylsemicarbazone. Finally, the latter (153 mg, 0.6 mmol) was heated at 100 °C in

50% ethanolic NaOH solution (10 M, 10%), followed by the addition of $K_3Fe(CN)_6$ in water (10 M, 10%). The reaction mixture was heated at 100 °C for 90 min. Subsequently, the reaction mixture was cooled in an ice bath and the solution was acidified with HCl (3 M) to afford the entitled compound **6**. Yield 45% (72 mg) ^{1}H NMR (DMSO-d_6) δ = 11.54 (s, 1H), 7.27 (d, J = 7.6 Hz, 1H), 7.12 (d, 1H), 7.05 (dd, J = 6.0 Hz, J = 2.0 Hz, 1H), 2.38 (tt, 1H), 2.27 (d, J = 4 Hz, 6H), 1.66 (m, 4H), 1.33, (m, 2H), 1.09 (m, 3H). ^{13}C-NMR (Acetone-d_6) δ = 138.7, 138.1, 132.3, 131.2, 129.5, 125.9, 35.7, 30.9, 26.5, 26.3, 19.7, 19.5. HRMS (m/z) 272.17576 calculated for $[M+H]^+$ = 272.17574. Purity (HPLC) 96%.

6.6.3 Biology

6.6.3.1 Binding Studies

[^{3}H]DPCPX and [^{3}H]ZM241385 were purchased from ARC Inc. St Louis, USA. [^{125}I]-AB-MECA was obtained from PerkinElmer Singapore PTE, Ltd. [^{3}H]PSB603 and [^{3}H]PSB11 were custom made for one of us (C.E.M.).

CHO cells expressing the human adenosine A_1 receptor were provided by Dr. Andrea Townsend- Nicholson, University College of London, UK. HEK 293 cells stably expressing the human adenosine A_{2A} and A_3 receptor were gifts from Dr. Wang (Biogen) and Dr. K.-N. Klotz (University of Würzburg, Germany), respectively. CHO cells expressing the human A_{2B} receptor were provided by Dr. Steve Rees (GlaxoSmithKline, UK).

All compounds made were tested in radioligand binding assays to determine their affinities at the human adenosine A_1, A_{2A}, A_{2B}, and the A_3 receptors.

6.6.3.2 Adenosine A_1 Receptor

Affinity at the A_1 receptor was determined on membranes from CHO cells expressing the human receptors, using [^{3}H]DPCPX as the radioligand. Membranes containing 5 µg of protein were incubated in a total volume of 100 µL of 50 mM Tris·HCl (pH 7.4) and [^{3}H]DPCPX (final concentration 1.6 nM) for 1 h at 25 °C in a shaking water bath.

Nonspecific binding was determined in the presence of 100 µM CPA. The incubation was terminated by filtration over pre-wetted Whatman GF/B filters under reduced pressure with a Brandel harvester. Filters were washed three times with ice-cold buffer and placed in scintillation vials. Emulsifier Safe (3.5 mL) was added, and after 2 h radioactivity was counted in a TriCarb 2900TR liquid scintillation counter.

6.6.3.3 Adenosine A_{2A} Receptor

At the A_{2A} receptor, affinity was determined on membranes from HEK 293 cells stably expressing this human receptor, using [^{3}H]ZM241385 as the radioligand. Membranes containing 40 µg of protein were incubated in a total volume of 100 µL of 50 mM Tris·HCl (pH 7.4) and [^{3}H]ZM241385 (final concentration 2.0 nM) for 2 h at 25 °C in a shaking water bath. Nonspecific binding was determined in the presence of 100 µM CGS. The incubation was terminated by filtration over pre-wetted Whatman GF/B filters under reduced pressure with a Brandel harvester. Filters were washed three times with ice-cold buffer and placed in scintillation vials. Emulsifier Safe (3.5 mL) was added, and after 2 h radioactivity was counted in a TriCarb 2900TR liquid scintillation counter.

6.6.3.4 Adenosine A_{2B} Receptor

At the A_{2B} receptor, radioligand displacement was determined on membranes from CHO cells stably transfected with human A_{2B} receptor, using [^{3}H]PBS603 as the radioligand. Membranes containing 15 µg of protein were incubated in a total volume of 100 µL of 50 mM Tris·HCl (pH 7.4), 1U/mL ADA, 0.1 w/v % CHAPS (pH 8.2 at 5 °C), and [^{3}H]PBS603 (final concentration 1.0 nM) for 2 h at 25 °C in a shaking water bath. Nonspecific binding was determined in the presence of 100 µM NECA. The incubation was terminated by filtration over pre-wetted Whatman GF/C filters under reduced pressure with a Brandel harvester. Filters were washed three times with ice-cold 50 mM Tris·HCl, pH7.4 + 0.1% BSA buffer and placed in scintillation vials. Emulsifier Safe (3.5 mL) was added, and after 5 h radioactivity was counted in a TriCarb 2900TR liquid scintillation counter.

6.6.3.5 Adenosine A_3 Receptor

The affinity at the A_3 receptor was measured on membranes from HEK 293 cells stably expressing the human A_3 receptor, using [^{3}H]PSB11 or [^{125}I]AB-MECA as the radioligand.

In the binding assays using [^{3}H]PSB11 as radioligand (final concentration 4 nM), membranes containing 50 µg of protein were incubated in a total volume of 100 µL of 55 mM Tris-HCl with 1 mM EDTA (pH 8 at 25^{o}C) for 2 h at 25 °C in a shaking water bath. Nonspecific binding was determined in the presence of 100 µM NECA.

In the binding assays using [^{125}I]AB-MECA as radioligand (final concentration 0.10 nM), membranes containing 25 µg of protein were incubated in a total volume of 100 µL of 50 mM Tris·HCl, 10 mM $MgCl_2$, 1 mM EDTA, 0.01% CHAPS (pH 7.4) for 1 h at 37 °C in a shaking water bath. Nonspecific binding was determined in the presence of 100 µM R-PIA. The incubation was terminated by filtration over pre-wetted Whatman GF/B filters under reduced pressure with a Brandel harvester. Filters were washed three times with ice-cold buffer and radioactivity was counted in a TriCarb 2900 TR liquid scintillation counter or in a Wallac 1470 Wizard gamma counter for [^{3}H]PSB11 or [^{125}I]AB-MECA, respectively.

6.7 Acknowledgements

We thank Prof. H. van Vlijmen for his useful suggestions on how to improve our computational method. This study was performed within the framework of the Dutch Top Institute Pharma, project number: D1-105.

6.8 Supporting Information

List of chemical structures generated using MOE method, schematic diagram of pharmacophore proposed by Chang et al[13], synthetic route schemes for all the compounds, and experimental details of the synthesis of the compounds **3a-3k** described in this chapter, their ^{1}H NMR and ^{13}C NMR spectroscopic data, HRMS data and HPLC data. This material is appended at the end of this chapter.

6.9 References

1. Fredholm, B. B.; IJzerman, A. P.; Jacobson, K. A.; Klotz, K. N.; Linden, J. International Union of Pharmacology. XXV. Nomenclature and classification of adenosine receptors. *Pharmacol. Rev.* **2001,** 53, 527-552.
2. Ralevic, V.; Burnstock, G. Receptors for purines and pyrimidines. *Pharmacol. Rev.* **1998,** 50, 413-492.
3. Jacobson, K. A.; Gao, Z. G. Adenosine receptors as therapeutic targets. *Nat. Rev. Drug Discov.* **2006,** 5, 247-264.
4. Muller, C. E. A(1)-adenosine receptor antagonists. *Expert Opin. Ther. Patents* **1997,** 7, 419-440.
5. Baraldi, P. G.; Tabrizi, M. A.; Gessi, S.; Borea, P. A. Adenosine receptor antagonists: Translating medicinal chemistry and pharmacology into clinical utility. *Chem. Rev.* **2008,** 108, 238-263.
6. Lameijer, E. W.; Kok, J. N.; Back, T.; IJzerman, A. P. The molecule evoluator. An interactive evolutionary algorithm for the design of drug-like molecules. *J. Chem Inf. Model.* **2006,** 46, 545-552.
7. Lameijer, E. W.; Tromp, R. A.; Spanjersberg, R. F.; Brussee, J.; IJzerman, A. P. Designing active template molecules by combining computational de novo design and human chemist's expertise. *J. Med. Chem.* **2007,** 50, 1925-1932.
8. Nicolaou, C. A.; Brown, N.; Pattichis, C. S. Molecular optimization using computational multi-objective methods. *Current Opinion in Drug Discovery & Development* **2007,** 10, 316-324.
9. Bender, A.; Young, D. W.; Jenkins, J. L.; Serrano, M.; Mikhailov, D.; Clemons, P. A.; Davies, J. W. Chemogenomic data analysis: Prediction of small-molecule targets and the advent of biological fingerprints. *Combinatorial Chemistry & High Throughput Screening* **2007,** 10, 719-731.
10. Bender, A.; Scheiber, J.; Glick, M.; Davies, J. W.; Azzaoui, K.; Hamon, J.; Urban, L.; Whitebread, S.; Jenkins, J. L. Analysis of Pharmacology Data and the Prediction of Adverse Drug Reactions and Off-Target Effects from Chemical Structure. *ChemMedChem* **2007,** 2, 861-873.
11. Morphy, R.; Kay, C.; Rankovic, Z. From magic bullets to designed multiple ligands. *Drug Discovery Today* **2004,** 9, 641-651.
12. Kazius, J.; McGuire, R.; Bursi, R. Derivation and Validation of Toxicophores for Mutagenicity Prediction. *J. Med. Chem* **2005,** 48, 312-320.
13. Chang, L. C. W.; Spanjersberg, R. F.; Kunzel, J. K. V.; Mulder-Krieger, T.; van den Hout, G.; Beukers, M. W.; Brussee, J.; IJzerman, A. P. 2,4,6-trisubstituted pyrimidines as a new class of selective adenosine A(1) receptor antagonists. *J. Med. Chem.* **2004,** 47, 6529-6540.
14. Ivanciuc, O. Applications of Support Vector Machines in Chemistry *Reviews in Computational Chemistry* **2007,** 23, 291.
15. Trautmann, H.; Weihs, C. On the distribution of the desirability index using Harrington's desirability function. *Metrika* **2006,** 63, 207-213

16. Nicolaou, C. A.; Apostolakis, J.; Pattichis, C. S. De Novo Drug Design Using Multiobjective Evolutionary Graphs. *J. Chem Inf. Model.* **2009,** 49, 295-307
17. Preuss, M.; Schönemann, L.; Emmerich, M. Counteracting genetic drift and disruptive recombination in (μpluskommaλ)-EA on multimodal fitness landscapes. In *Proceedings of the 2005 conference on Genetic and evolutionary computation*, ACM: Washington DC, USA, 2005; pp 865-872
18. Kruisselbrink, J. W.; Aleman, A.; Emmerich, M.; IJzerman, A. P.; Bender, A.; Baeck, T.; van der Horst, E. Enhancing search space diversity in multi-objective evolutionary drug molecule design using niching. In *Proceedings of the 11th Annual conference on Genetic and evolutionary computation*, 2009; pp 217–224.
19. Bender, A.; Glen, R. C. Molecular similarity: a key technique in molecular informatics. *Organic & Biomolecular Chemistry* **2004,** 2, 3204-3218
20. Murdoch, R.; Tully, W. R.; Westwood, R. Synthesis of [1,2,4]Triazoloquinazolinones and Imidazoquinazolinones. *J. Heterocycl. Chem.* **1986,** 23, 833-841.
21. El-Tombary, A. A.; Ismail, K. A.; Aboulwafa, O. M.; Omar, A.; El-Azzouni, M. Z.; El-Mansoury, S. T. Novel triazolo[4,3-a]quinazolinone and bis-triazolo[4,3-a : 4,3 '-c]quinazolines: synthesis and antitoxoplasmosis effect. *Farmaco* **1999,** 54, 486-495.
22. Ferraris, D.; Ko, Y. S.; Pahutski, T.; Ficco, R. P.; Serdyuk, L.; Alemu, C.; Bradford, C.; Chiou, T.; Hoover, R.; Huang, S.; Lautar, S.; Liang, S.; Lin, Q. A.; Lu, M. X. C.; Mooney, M.; Morgan, L.; Qian, Y. Z.; Tran, S.; Williams, L. R.; Wu, Q. Y.; Zhang, J.; Zou, Y. N.; Kalish, V. Design and synthesis of poly ADP-ribose polymerase-1 inhibitors. 2. Biological evaluation of aza-5[H]-phenanthridin-6-ones as potent, aqueous-soluble compounds for the treatment of ischemic injuries. *J. Med. Chem.* **2003,** 46, 3138-3151.
23. Laufer, R. S.; Dmitrienko, G. I. Diazo group electrophilicity in kinamycins and lomaiviticin A: Potential insights into the molecular mechanism of antibacterial and antitumor activity. *J. Am. Chem. Soc.* **2002,** 124, 1854-1855.
24. Sridhar, M.; Rao, R. M.; Baba, N. H. K.; Kumbhare, R. M. Microwave accelerated Gewald reaction: synthesis of 2-aminothiophenes. *Tetrahedron Lett.* **2007,** 48, 3171-3172.
25. de Matos, P.; Alcantara, R.; Dekker, A.; Ennis, M.; Hastings, J.; Haug, K.; Spiteri, I.; Turner, S.; Steinbeck, C. Chemical Entities of Biological Interest: an update. *Nucl. Acids Res.* **2010,** 38, D249-254
26. Irwin, J. J.; Shoichet, B. K. ZINC - A free database of commercially available compounds for virtual screening. *J. Chem Inf. Model.* **2005,** 45, 177-182.
27. Bemis, G. W.; Murcko, M. A. The Properties of Known Drugs. 1. Molecular Frameworks. *J. Med. Chem.* **1996,** 39, 2887-2893.
28. Bemis, G. W.; Murcko, M. A. Properties of Known Drugs. 2. Side Chains. *J. Med. Chem.* **1999,** 42, 5095-5099.
29. Ertl, P.; Rohde, B.; Selzer, P. Fast calculation of molecular polar surface area as a sum of fragment-based contributions and its application to the prediction of drug transport properties. *J. Med. Chem.* **2000,** 43, 3714-3717.

30. *Scitegic Pipeline Pilot*, 6.1.5.0 Student Edition; Accelrys, Inc.: San Diego, CA, 2007.
31. *Molecular Operating Environment*, 2008.10; Chemical Computing Group: Montreal, Quebec, Canada, 2008.
32. Bender, A.; Jenkins, J. L.; Scheiber, J.; Sukuru, S. C. K.; Glick, M.; Davies, J. W. How Similar Are Similarity Searching Methods? A Principal Component Analysis of Molecular Descriptor Space. *J. Chem Inf. Model.* **2009,** 49, 108-119.
33. Kruisselbrink, J.; Emmerich, M.; Bäck, T.; Bender, A.; IJzerman, A.; van der Horst, E. Combining Aggregation with Pareto Optimization: A Case Study in Evolutionary Molecular Design. In *Evolutionary Multi-Criterion Optimization*, Springer Berlin / Heidelberg: 2009; Vol. 5467, pp 453-467.
34. Shir, O.; Preuss, M.; Naujoks, B.; Emmerich, M. Enhancing Decision Space Diversity in Evolutionary Multiobjective Algorithms. In *Evolutionary Multi-Criterion Optimization*, 2009; pp 95-109
35. Hermecz, I.; Horvath, A.; Vasvaridebreczy, L.; Meszaros, Z. Nitrogen-Bridgehead compounds .40. Cyclization in phosphoryl chloride polyphosphoric acid mixture. *Synthesis* **1984**, 152-158.

6.10 Supporting Information

Table of contents:

Figure S1. Chemical structures of scaffolds generated by multi-objective evolutionary design.

Figure S2. Schematic representation of reported pharmacophore for A_1 AR.

Scheme S1-S5. Synthetic routes to compounds **1-6.**

S3. Experimental procedures and spectral data of compounds **3a-3k**

Figure S1. Chemical structures of scaffolds generated by multi-objective evolutionary (MOE) design. Green spheres denote hydrophobic substituents (mostly alkyl chains) and red spheres denote hydrogen donor groups (mostly amino and hydroxo groups).

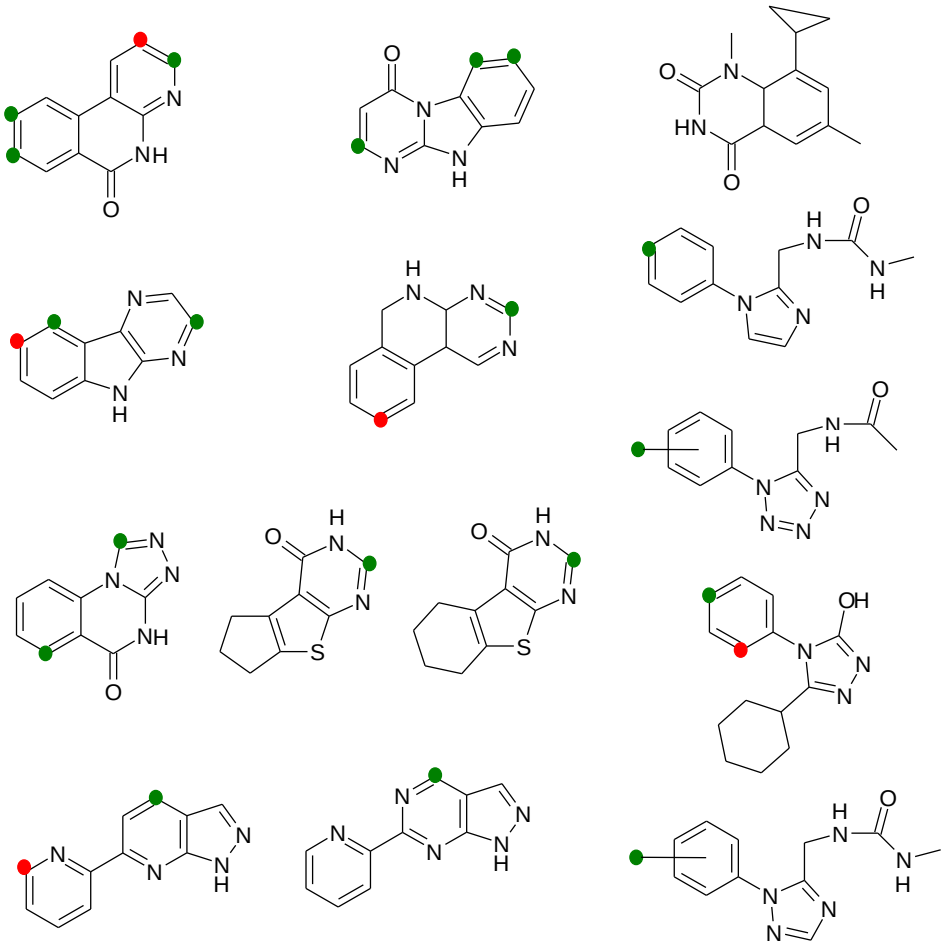

Figure S2. Schematic diagram of pharmacophore proposed by Chang *et al* (J Med Chem 47 (2004) 6529). At the center is the aromatic core which is surrounded by three lipophilic regions, Lip_1, Lip_2, and Lip_3. Below the aromatic core are the hydrogen bond acceptor and donor region, Acc_1 and Don_1, respectively. On the right of the aromatic core, a second hydrogen bond acceptor, Acc_2, is located.

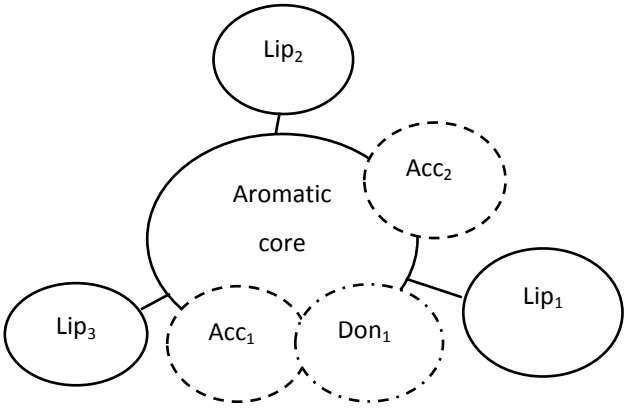

Scheme S1. Synthetic route to [1,2,4]Triazolo[4,3-a]quinazolin-5-one (**1**) (i) Hydrazine hydrate, K_2CO_3, 2h reflux, pH 7 with AcOH (ii) Formic acid, 95 °C, 4 h.

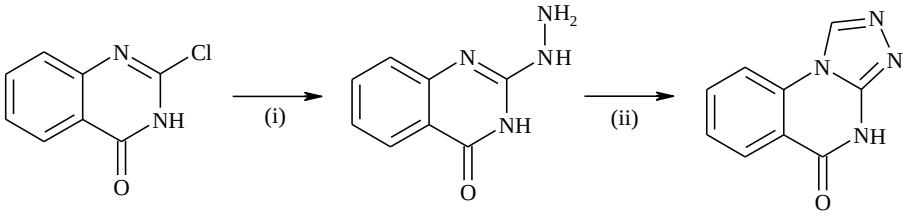

1.

Scheme 2. Synthetic route to 4-Aza-5[H]-phenanthridin-6-one (**2**); (i) $NH(^iPr)_2$, Et_3N, Et_2O, 0 °C; (ii) s-BuLi, THF, $B(OMe)_3$, -78 °C; (iii) $Pd(OAc)_2$, PPh_3, K_2CO_3, 2-amino-3-bromopyridine, toluene/EtOH MW 160 °C, 60 min; (iv) LDA, THF, -78 °C.

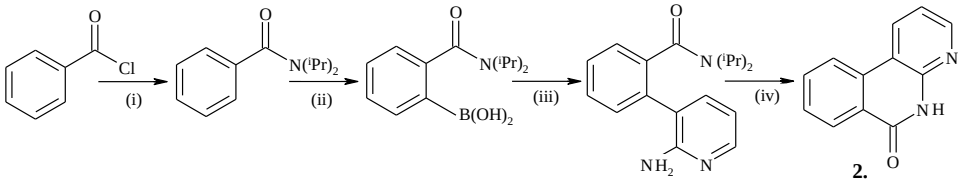

2.

Scheme S3. Synthetic route to 2-methylpyrimido[1,2-*a*]benzimidazol-4(10*H*)-one (**3**) (i) $POCl_3$ / Phosphoric acid (PPA), 130 °C.

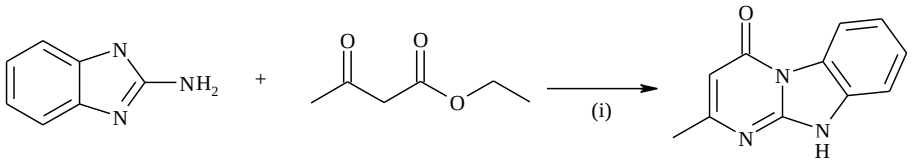

3.

Scheme S4. Synthetic route to 3,5,6,7-tetrahydro-4*H*-cyclopenta[4,5]thieno[2,3-*d*]pyrimidin-4-one (**4**) and 5,6,7,8-tetrahydro[1]benzothieno[2,3-*d*]pyrimidin-4(3*H*)-one (**5**) (i) KF/alumina, elemental S, malonitrile, EtOH,100 °C, 5 min; (ii) formic acid 110 °C MW 5 min.

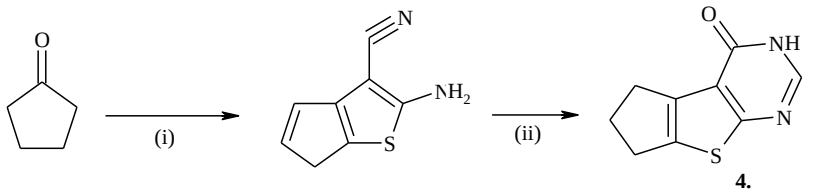

4.

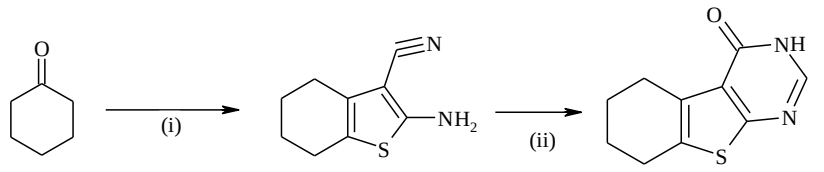

5.

Scheme S5. Synthetic route to 5-cyclohexyl-4-(3,4-dimethylphenyl)-2,4-dihydro-3*H*-1,2,4-triazol-3-one (**6**); (i) cyclohexanecarbaldehyde, EtOH reflux; (ii) 100 °C 50% ethanolic NaOH solution, $K_3[Fe(CN)_6]$ 90 min.

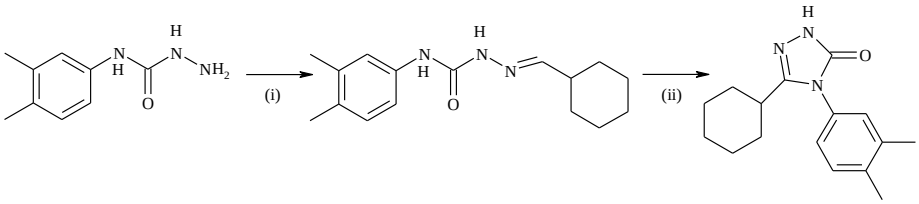

S3. General procedure for the preparation of compounds 3a-3k under microwave conditions.

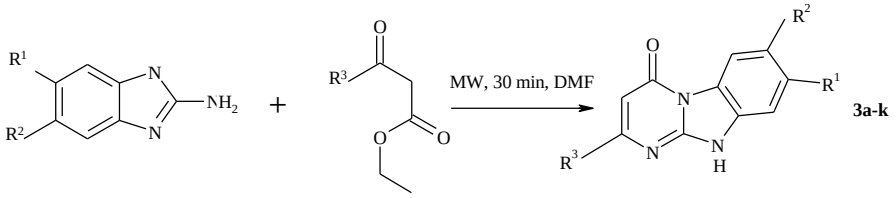

To a solution of 2-aminobenzimidazole or 2-amino-5,6-dimethylbenzimidazole in DMF (3 mL), the corresponding β-keto-ester was added in equimolar amounts. The reaction mixture was stirred and heated at 165 °C under microwave conditions for 30 min. A solid was formed upon cooling, which was filtered and washed with cold H_2O, MeOH and Et_2O. The filtrate was concentrated under reduced pressure and extracted with EtOAc. Subsequently, the organic layers were combined, dried over $MgSO_4$, concentrated and purified using chromatography on SiO_2.

2-Isopropylpyrimido[1,2-*a*]benzimidazol-4(10*H*)-one (3a) Yield: 40% (127 mg) ^{1}H NMR (DMSO-d_6) δ = 12.85 (s br, 1H), 8.39 (d, J = 8.0 Hz, 1H,), 7.49-7.41 (m, 2H), 7.29 (d, J = 7.2 Hz, 1H), 2.83 (m, 1H), 1.23 (d, J = 6.8 Hz, 6H) ppm. ^{13}C-NMR (DMSO-d_6) δ = 159.7, 148.9, 126.2, 121.5, 115.3, 112.5, 96.4, 34.4, 21.4 ppm. Anal. Calcd for [$C_{13}H_{13}N_3O$]: C, 68.7; H, 5.8; N, 18.5. Found C, 68.6; H, 5.9; N, 18.6. HRMS (m/z) = 228.11309 calculated for $[M+H]^+$ = 228.11314.

2-Propylpyrimido[1,2-*a*]benzimidazol-4(10*H*)-one (3b) Yield: 43% (137 mg) ^{1}H NMR (DMSO-d_6) δ = 12.73 (s br, 1H), 8.37 (d, J = 8.0 Hz, 1H), 7.50 (d, J = 8.0 Hz, 1H), 7.43 (t, J = 7.2 Hz, 1H), 7.28 (t, J = 8.0 Hz, 1H), 5.84 (s,1H), 2.53 (t, J = 7.2 Hz, 2H), 1.69 (m, 2H), 0.93 (t, J = 7.6 Hz, 3H) ppm. ^{13}C-NMR (DMSO-d_6) δ = 159.4, 148.6, 125.6, 121.4, 115.2, 113.2, 98.2, 37.3, 21.1, 13.5 ppm. HRMS (m/z) = 228.11310 calculated for $[M+H]^+$ = 228.11314. Purity (HPLC) 99%

2-Cyclohexylpyrimido[1,2-*a*]benzimidazol-4(10*H*)-one (3c) Yield: 57% (147 mg) ^{1}H NMR (DMSO-d_6) δ = 12.81 (s br, 1H), 8.38 (d, J = 8.0 Hz, 1H), 7.48 (d, J = 7.6 Hz, 1H), 7.43 (t, J = 7.2 Hz, 1H), 7.28 (t, J = 7.2 Hz, 1H), 5.83 (s, 1H), 1.82 (dd, J = 12.0, 4H), 1.68 (d, J = 11.2 Hz, 1H), 1.45 (q, 2H), 1.30 (q, 2H), 1.22 (m, 2H)ppm. ^{13}C-NMR (DMSO-d_6) δ = 159.9, 148.9, 125.9, 121.6, 115.4, 112.7, 96.8, 65.0, 49.8, 46.8, 44.4, 31.4, 27.8, 25.9, 25.6, 25.1 ppm. HRMS (m/z) = 268.14448 calculated for $[M+H]^+$ = 268.14444. Purity (HPLC) 99%

2-Phenylpyrimido[1,2-*a*]benzimidazol-4(10*H*)-one (3d) Yield: 31% (302 mg) ^{1}H NMR (DMSO-d_6) δ = 13. 1 (s br, 1H), 8.47 (d, J = 8.0 Hz, 1H), 8.11 (m, 2H), 7.49 (m, 5H), 7.35 (m, 1H), 6.62 (s, 1H) ppm. ^{13}C-NMR (DMSO-d_6) δ = 159.8, 149.6, 136.9, 130.3, 128.7, 126.7, 126.2, 121, 8, 115.7, 111.02, 97.1 ppm. HRMS (m/z) = 262.09752 calculated for $[M+H]^+$ = 262.09749. Purity (HPLC) 99%

2-(4-pyridyl)pyrimido[1,2-*a*]benzimidazol-4(10*H*)-one (3e) Yield: 59% (350 mg) ^{1}H NMR (DMSO-d_6) δ = 13.2 (s br, 1H), 8.72 (d, J = 6.4 Hz, 2H), 8.48 (d, J = 10.4 Hz, 1H), 8.06 (d, J = 6.4 Hz, 2H), 7.51 (d, J = 5.2 Hz, 2H), 7.36 (m, 1H), 6.83 (s, 1H) ppm. ^{13}C-NMR (DMSO-d_6) δ = 159.8, 158.1, 150.4, 149.8, 144.4, 130.7, 126.5. 125.8, 122.1, 121.1, 115,8, 111.2, 98.5 ppm. HRMS (m/z) = 263.09263 calculated for $[M+H]^+$ = 263.09274. Purity (HPLC) 99%

2-Methyl-7,8-dimethylpyrimido[1,2-*a*]benzimidazol-4(10*H*)-one (3f) Yield: 26% (71 mg) ^{1}H NMR (DMSO-d_6) δ = 12.6 (s br, 1H), 8.16 (s, 1H), 7.29 (s, 1H), 5.81 (s, 1H), 2.33 (s, 6H), 2.27 (s, 3H) ppm. ^{13}C-NMR (DMSO-d_6) δ = 159.2, 148.3, 134.3, 129.8, 124.8, 115.6, 113.3, 98.6, 22.3, 20.0, 19.8 ppm. Anal. Calcd for [$C_{13}H_{13}N_3O$]: C, 68.7; H, 5.8, N, 18.5. Found C, 68.2; H, 5.6, N, 18.4. HRMS (m/z) = 228.11307 calculated for $[M+H]^+$ = 228.11307.

2-Isopropyl-7,8-dimethylpyrimido[1,2-*a*]benzimidazol-4(10*H*)-one (3g) Yield: 30% (91 mg) ^{1}H NMR (DMSO-d_6) δ = 12.72 (s br, 1H), 8.18 (s, 1H), 7.25 (s, 1H), 5.85 (s, 1H), 2.80 (m, 1H), 2.34 (s, 6H), 1.22 (d, J = 6.8Hz, 6H) ppm. ^{13}C-NMR (DMSO-d_6) δ = 159.6, 134.5,

129.9, 115.7, 96.5, 34.7, 21.5, 19.9, 19.8 ppm. HRMS (m/z) = 256.14446 calculated for $[M+H]^+$ = 25614444. Purity (HPLC) 99%

2-Propyl-7,8-dimethylpyrimido[1,2-*a*]benzimidazol-4(10*H*)-one (3h) Yield: 41% (124 mg) ^{1}H NMR (DMSO-d_6) δ = 12.63 (s br, 1H), 8.16 (s, 1H), 7.26 (s, 1H), 5.81 (s, 1H), 2.33 (s, 6H), 1.67 (m, 2H), 0.92 (t, J = 7.6 Hz, 3H) (peak below dmso corresponding to CH_2) ppm. ^{13}C-NMR (DMSO-d_6) δ = 159.3, 134.3, 129.8, 115.6, 98.4, 37.9, 21.2, 19.9, 19.8, 13.6 ppm. HRMS (m/z) = 256.14445 calculated for $[M+H]^+$ = 256.14444. Purity (HPLC) 98%

2-Cyclohexyl-7,8-dimethylpyrimido[1,2-*a*]benzimidazol-4(10*H*)-one (3i) Yield: 37% (132 mg) ^{1}H NMR ($CDCl_3$) δ = 8.39 (s, 1H), 7.29 (s, 1H), 6.01 (s, 1H), 2.64 (t, J = 10.8 Hz, 1H), 2.08 (d, J = 13.2 Hz, 2H), 1.90 (d, J = 12.4 Hz, 2H), 1.79 (d, J = 12.8 Hz, 1H), 1.48 (m, 4H), 1.31 (t, J = 11.6 Hz, 1H) ppm. ^{13}C-NMR ($CDCl_3$) δ = 159.9, 148.4, 133.8, 129.4, 123.9, 115.6, 111.4, 96.6, 44.6, 31.1, 25.4, 25.2, 19.6, 19.2 ppm. HRMS (m/z) = 296.17586 calculated for $[M+H]^+$ = 296.17574. Purity (HPLC) 96%

2-Phenyl-7,8-dimethylpyrimido[1,2-*a*]benzimidazol-4(10*H*)-one (3j) Yield: 37% (130 mg) ^{1}H NMR (DMSO-d_6) δ = 12.9 (s br, 1H), 8.26 (s, 1H), 8.10 (d, J = 6.0 Hz, 2H), 7.50 (d, J = 6.8 Hz, 3H), 7.29 (s, 1H), 6.60 (s, 1H), 2.37 (s, 6H) ppm. ^{13}C-NMR (DMSO-d_6) δ = 159.7, 135.0, 130.3, 130.2, 128.7, 126.9, 116.0, 111.4, 96.8, 19.9, 19.8 ppm. HRMS (m/z) = 290.12883 calculated for $[M+H]^+$ = 290.12879. Purity (HPLC) 98%

2-(4-pyridyl)-7,8-dimethylpyrimido[1,2-*a*]benzimidazol-4(10*H*)-one (3k) Yield: 68% (365 mg) ^{1}H NMR (DMSO-d_6) δ = 13.1 (s br, 1H), 8.72 (d, J = 5.1 Hz, 2H), 8.30 (s, 1H), 8.05 (d, J = 4.8 Hz, 2H), 7.31 (s, 1H), 6.79 (s, 1H), 8.27 (s, 6H) ppm. ^{13}C-NMR (DMSO-d_6) δ = 149.3, 134.1, 129.4, 120.0, 115.1, 110.5, 97.2, 19.0, 18.8 ppm. HRMS (m/z) = 291.12394 calculated for $[M+H]^+$ = 291.12404. Purity (HPLC) 96%.